

RESEARCH

Open Access



# Evaluation of the impact of customized serum-free culture medium on the production of clinical-grade human umbilical cord mesenchymal stem cells: insights for future clinical applications

Lan Zhao<sup>1†</sup>, Beibei Ni<sup>2†</sup>, Jinqing Li<sup>3†</sup>, Rui Liu<sup>1</sup>, Qi Zhang<sup>2</sup>, Zhuangbin Zheng<sup>1</sup>, Wenjuan Yang<sup>4\*</sup>, Wei Yu<sup>1\*</sup> and Lijun Bi<sup>1\*</sup> 

## Abstract

**Background** The selection of suitable culture medium is critical for achieving good clinical outcomes in cell therapy. To support the commercial application of stem cell therapy, customized culture media not only need to promote stem cell proliferation, but also need to save costs and meet industrial requirements for inter-batch consistency, efficacy, and biosafety. In this study, we developed a series of serum-free media (SFM) and elucidated the effects between different SFM, as well as between SFM and serum-containing media (SCM), on human umbilical cord mesenchymal stem cells (hUC-MSCs) phenotype and function. We analyze and emphasize from the perspectives of clinical and commercial application why research on customized culture media is critical for the success of enterprises developing novel cellular therapeutics.

**Methods** We cultured hUC-MSCs with identical cell seeding densities in different formulations of SFM and SCM until passage 10 and examined the changes in cell phenotype and function. We analyzed the results with the commercial application requirements of the cellular therapy industry to assess the potential impact of customized culture media on inter-batch consistency, efficacy, stability, biosafety, and cost-effectiveness of industrial-scale cell production.

**Results** hUC-MSCs cultured in SCM and SFM exhibit consistent cell morphology and surface molecule expression, but hUC-MSCs cultured in SFM demonstrate higher activity, superior proliferative capacity, and greater stability. Furthermore, hUC-MSCs cultured in different SFM exhibit differences in cell activity, proliferative capacity, senescent rate, and S/M ratio of cell cycle, while maintaining a normal karyotype after long-term in vitro cultivation. Moreover,

<sup>†</sup>Lan Zhao, Beibei Ni, Jinqing Li have contributed equally to this work.

\*Correspondence:

Wenjuan Yang

yangwj28@mail.sysu.edu.cn

Wei Yu

yu\_wei@gzlab.ac.cn

Lijun Bi

bi\_lijun@gzlab.ac.cn; bilijun2024@163.com

Full list of author information is available at the end of the article



we found that hUC-MSCs cultured in different media exhibit variations in paracrine capacity and in their support of hematopoietic stem cell (HSC) self-renewal.

**Conclusion** Considering the substantial funding and time required for cell-based drug development, our results underscore the importances of comprehensively optimizing the composition of medium for the specific disease prior to conducting clinical trials of cell-based therapies. The criteria for selecting culture medium should be based on the requirements of the target disease for cellular function. In addition, we provide a way to formulate different customized SFM, which is beneficial for the development of cell therapy industry.

**Keywords** Stem cell therapy, SFM, hUC-MSCs

## Background

Mesenchymal Stem/Stromal Cells (MSCs) have been well demonstrated by numerous *in vivo* studies to possess potential clinical applications for various diseases due to their role in immunoregulation, anti-inflammatory, and multipotent differentiation potential [1–5]. To facilitate the rapid translation and implementation of this novel therapy, countries worldwide are prioritizing and supporting the clinical application of MSCs as a key area for development [6, 7]. Currently, there are more than 1200 registered MSCs clinical trials and over 60,000 publications on MSCs [8, 9]. With breakthroughs in the potential mechanisms and therapeutic strategies of MSCs in treating various diseases, the cell therapy industry is expected to bring significant market value in the foreseeable future, while also assisting humanity in achieving better health outcomes [10, 11].

Cell culture media specifically designed to support the growth of MSCs are critical for the clinical application of MSCs [12, 13]. They provide the necessary nutrients for cell growth, create a suitable environment, and shape the phenotype and function of the cells [14, 15]. The majority of MSCs products use a combination of cluster of differentiation (CD) markers, trilineage differentiation potential, and cell morphology as identification criteria for MSCs [16–19]. According to International Society for Cellular Therapy (ISCT) in 2006, the MSCs should express high CD90, CD73, and CD105 ( $\geq 95\%$ ) while lacking expression of CD45, CD34, CD14, CD19, and HLA-DR ( $\leq 2\%$ ) markers [20]. However, while many MSCs cultured *in vitro* using general-purpose media meet these criteria, they may not be sufficient to define MSCs products used for clinical disease therapy. On one hand, media that only support lower cell passage numbers may not align with the goal of large-scale clinical MSCs production [21]. On the other hand, MSCs produced in different media may exhibit variations in activity, functionality, and other characteristics [22]. These differences could have significant implications for the development of MSCs products and may even determine the outcomes of subsequent disease treatments. Considering that cultured

MSCs will be applied in clinical disease therapy rather than scientific research, customized high-quality media should meet the requirements for inter-batch consistency, efficacy, passage stability, biological safety, and cost-effectiveness in industrial-scale cell production.

Despite the limitations of using SCM for *ex vivo* MSCs expansion for clinical trials, including potential risks such as unknown viral contamination, immunological reactions, and affecting cell batch stability, many companies still employ this xenogenic additive [23–25]. Compared to SCM, SFM offer greater advantages in cultivating clinical-grade MSCs because it lack xenogeneic components and ensure stable quality [26, 27]. However, whether SFM can stably support long-term MSCs growth compared to SCM, and whether MSCs cultured in different SFM exhibit different characteristics, lack systematic research.

In this study, we evaluated the impact of different types and formulations of culture media on inter-batch consistency, cost-effectiveness, passability stability, biological safety, and efficacy required for industrial scale cell production. By systematically comparing the biological characteristics and functionalities of hUC-MSCs in different culture media, this study aimed to assist MSCs product developers gain a deeper understanding of why the selection and optimization of disease based culture media significantly impact the development of clinical applications of MSCs. The results indicated that while hUC-MSCs cultured in different types and formulations of culture media all meet the ISCT criteria for MSC identification, variations exist in cell phenotype and function, which may influence the therapeutic outcomes of subsequent diseases. Considering the differences in disease mechanisms, these findings suggested that appropriate culture media should be chosen based on the specific type of disease being treated, rather than solely relying on classical MSC identification methods such as cell morphology, surface markers, and differentiation potential. Besides, optimizing culture conditions for specific diseases during the preclinical stage of MSCs product development can effectively reduce both the time and costs of the project, thereby facilitating the commercial application of MSCs

products. This approach enables the development of MSCs products tailored to specific diseases.

**Methods**

**Media preparation**

The formulation and quality control of different SFM and SCM were illustrated in Table 1. All media were prepared under Good Manufacturing Practice (GMP) conditions, followed by testing for pH, osmolarity, endotoxin, fungi and bacteria. SFM were formulated by basal media, such as  $\alpha$ -MEM (PM150421, PROCELL) or UltraCULTURE Serum-free media (BP12-725F, LONZA), supplemented with serum substitutes of non-xenogeneic origin and other additives. SCM were formulated by classical  $\alpha$ -MEM or RPMI-1640 supplemented with 10% fetal bovine serum (FBS).

**Isolation and culture of hUC-MSCs**

Informed consent was obtained from all individuals prior to the collection of fresh umbilical cord (UC) from full-term births. The fresh UC was washed with injectable sodium chloride to clear its surface and remove residual blood within the cord. The veins and arteries were removed using forceps, and Wharton’s jelly was isolated, then cut into small pieces measuring 1–2 mm<sup>2</sup>. The Wharton’s jelly was placed into centrifuge tubes and supplemented with pre-prepared complete culture medium. After thorough mixing, the cells were seeded into T75 culture flasks. Half of the culture medium was refreshed every 5 days based on the cell growth status until reaching 80% confluency, at which point passaging was performed.

When passaging was required, cells were rinsed with PBS and then treated with 0.05% trypsin (25200072, Gibco) at 37 °C for the specified duration. The harvested hUC-MSCs were expanded to the 10th passage at a

**Table 1** The formulation and quality control of SFM and SCM

Formulation					Quality control				
	Components	Company	Catalog number	Concentration	PH	Osmolarity (mOsmol kg <sup>-1</sup> )	Endotoxin (EU/ml)	Fungi	Bacteria
SFM1	$\alpha$ -MEM	Procell	PM 150421	94 vol%	7.46 ± 0.46	301 ± 5	< 2	Negative	Negative
	Recombinant human insulin	Yuanye Biotech	11061-68-0	10 mg/L					
	Recombinant human transferrin	Yuanye Biotech	S23602	5.5 mg/L					
	Recombinant human transforming growth factor- $\beta$ 1	PeproTech	AF10021C	0.005 mg/L					
	Sodium selenite	Nanjing Reagent	10102-18-8	0.0067 mg/L					
	L-glutamine	Procel	PB180420	1 vol%					
	Human platelet lysate	Sexton	PL-NH-100	5 vol%					
SFM2	$\alpha$ -MEM	Procell	PM150421	94 vol%	7.56 ± 0.66	300 ± 8	< 2	Negative	Negative
	L-glutamine	Procel	PB180420	1 vol%					
	Human platelet lysate	Sexton	PL-NH-100	5 vol%					
SFM3	$\alpha$ -MEM	Procell	PM150421	94 vol%	7.88 ± 0.52	297 ± 6	< 2	Negative	Negative
	L-glutamine	Procel	PB180420	1 vol%					
	UltraGRO™-Advanced	HELIOS	HPCFDCRL50	5 vol%					
SFM4	UltraCULTURE Serum-free Medium	LONZA	BP12-725F	97 vol%	7.32 ± 0.78	304 ± 5	< 2	Negative	Negative
	GlutMAX-I	Procell	PB180420	1 vol%					
	Ultroser G Serum Substitute	PALL	15950-017	2 vol%					
SCM1	$\alpha$ -MEM	Procell	PM150421	89 vol%	7.47 ± 0.42	293 ± 9	< 2	Negative	Negative
	L-glutamine	Procel	PB180420	1 vol%					
	FBS	BI	04-001-1ACS	10 vol%					
SCM2	RPMI-1640	Procel	PM150110	89 vol%	7.43 ± 0.55	289 ± 9	< 2	Negative	Negative
	L-glutamine	Procel	PB180420	1 vol%					
	FBS	BI	04-001-1ACS	10 vol%					

density of 6000–7000 cells/cm<sup>2</sup> in the respective culture medium, and physiological and functional parameters of cells at different passages were investigated.

#### **Analysis of cell morphology, size, activity, quantity, and doubling time**

hUC-MSCs were cultured in customized SFM and SCM to corresponding passages, and cell viability was assessed using trypan blue staining (15250-061, Gibco). When cells reached approximately 80% confluency at the respective passages, optical microscopy was employed to record cell morphology. At indicated passages, cell morphology was also analyzed by the aspect ratio of cell length to width (L : W). The population doubling time (PDT) was evaluated using the following formula:  $PDT = T * [\lg_2 / (\lg N_t - \lg N_0)]$ , where T represents the culture time, N<sub>0</sub> denotes the initial cell number after seeding, and N<sub>t</sub> signifies the cell number after t hours of culture. The cumulative total cell count at different passages for cells cultured in customized medium was calculated by multiplying the initial cell number of  $1 * 10^5$  cells by the average expansion factor observed for each passage.

#### **Analysis of cell cryopreservation and recovery**

The hUC-MSCs from passages 4 (P4) and 9 (P9) were harvested by trypsinization, washed, and centrifuged. Subsequently, the cells were resuspended in complete culture medium supplemented with 20% CryoPur-D (CD-100, OriGen). Then the cells were gradually cooled to –80 °C using a programmed cooling protocol before being transferred to liquid nitrogen for long-term storage. After 3 to 6 months of cryopreservation, cells were thawed at 37 °C and used for subsequent experiments. Cell viability, multiple increase, and PDT were recorded before and after cryopreservation.

#### **Flow cytometry analysis of hUC-MSCs phenotype and cell cycle**

hUC-MSCs from P5 and P10 were harvested by trypsinization and utilized for cell surface marker staining (anti-CD14-APC-eFluor506: 47-0149-42, eBioscience; anti-CD19-PE-Cyanine5.5: 35-0198-42, eBioscience; anti-CD34-APC: 17-0349-42, eBioscience; anti-CD45-PE-Cyanine7: 25-0459-42, eBioscience; anti-HLADR-eFluor506: 69-9956-42, eBioscience; anti-CD73-FITC: 11-0739-42, eBioscience; anti-CD90-PE: 12-0909-42, eBioscience; anti-CD105-eFluor450: 48-1057-42, eBioscience). Data analysis was conducted using CytoFlex (Beckman Coulter). For cell cycle analysis, cells were fixed in 70% pre-chilled ethanol for 12 h, followed by centrifugation, cell washing, and subsequent staining with propidium iodide (PI) staining solution prepared

according to the instructions of the kit (C1052, Beyotime Biotechnology) for 30 min.

#### **Analysis of the differentiation potential of hUC-MSCs into three lineages**

The hUC-MSCs were differentiated towards osteogenic (HUXUC-90021, Cyagen), adipogenic (HUXUC-90031, Cyagen), and chondrogenic (HUXUC-90041, Cyagen) lineages using Cyagen's differentiation kits.

For osteogenic differentiation, hUC-MSCs of P4 and P9 were seeded at a density of 6000 cells/cm<sup>2</sup> in 6-wells pre-coated with 0.1% gelatin and cultured with their respective culture medium. When the cell confluence reached 70%, change the culture medium to osteogenic induction medium (HUXUC-90021, Cyagen). In parallel, undifferentiated MSCs were cultured in their respective complete medium as negative controls. The medium was changed every 3 days. After 21 days of differentiation, cells were washed with PBS, fixed in 4% Polyformaldehyde (PFA) for 30 min, washed with PBS, and then stained with 2% Alizarin Red S solution for 10 min. After washing with PBS, the images of osteogenesis staining were captured under a microscope.

For adipogenic differentiation, hUC-MSCs of P4 and P9 were seeded at a density of 6000 cells/cm<sup>2</sup> in 6-wells pre-coated with 0.1% gelatin and cultured with their respective culture medium. When the cell confluence reached 100%, change the culture medium to adipogenesis induction medium (HUXUC-90031, Cyagen). Replace the medium every 3–4 days for 28 days. In parallel, undifferentiated MSCs were cultured in their respective complete medium as negative controls. After adipogenic induction, cells were washed with PBS, fixed in 4% PFA for 30 min, washed with PBS, and then stained with Oil Red O for 30 min. After washing with PBS, the images of adipogenesis staining were captured under a microscope.

For chondrogenic differentiation, hUC-MSCs of P4 and P9 were seeded at a density of  $5 * 10^5$  into 15 mL centrifuge tubes with 0.5 ml chondrogenic induction medium (HUXUC-90041, Cyagen). After centrifugation at 200 g, loosen the tube lids slightly to allow for gas exchange. After 24 h, cell aggregates formed clusters. Gently tap the bottom of the centrifuge tube to dislodge the spheres from the bottom and allow them to grow in suspension. Replace the culture medium every 2 days. After 14 days of culture, the cell spheroids were collected and fixed in 4% PFA, dehydrated using 30% sucrose, embedded in optimal cutting temperature compound (OCT, a water-soluble mixture of polyethylene glycol and polyvinyl alcohol) (4583, SAKURA), rapidly frozen with liquid nitrogen, and then sectioned. The sections were then further stained with Alcian Blue. Undifferentiated MSCs

were cultured in their respective complete medium as negative controls.

#### Senescence of hUC-MSCs analysis

When cells reached the indicated passages, the senescence status of hUC-MSCs was assessed and analyzed using the  $\beta$ -galactosidase detection kit (C0602, Beyotime Biotechnology). Briefly,  $3 \times 10^4$  cells were seeded into 12-well plates and cultured for 3 days in the customized SFM and SCM. After removing the culture medium, cells were washed once with PBS and fixed with 1 ml of fixation solution at room temperature for 15 min. Following fixation solution removal, cells were washed three times with PBS and stained with  $\beta$ -galactosidase staining solution prepared according to the kit instructions. The culture plates were sealed with plastic wrap to prevent evaporation and then placed in a 37 °C incubator overnight. Cell senescence status was observed under an optical microscope.

#### Analyzing the growth kinetics of hUC-MSCs

P5 and P10 hUC-MSCs were used to analyze the growth kinetics. Briefly, cells from passages P4 or P9 were harvested by trypsin digestion and seeded at a density of  $1.5 \times 10^3$  cells per well into a 24-well plate. At predetermined time points, cell proliferation was assessed by trypan blue staining (15250-061, Gibco) and cell counts were recorded to generate cell proliferation curves. The population proliferative level of logarithmic growth phase cells (PPL) was calculated using the following formula:  $PPL = (N_t - N_0)/T$ , where  $N_t$  represents the cell count at the onset of stable growth,  $N_0$  denotes the cell count at the initiation of exponential growth, and  $T$  represents the time interval from  $N_0$  to  $N_t$ .

#### Chromosome karyotype analysis

To assess the possibility of chromosomal abnormalities, P5 and P10 passages of hUC-MSCs cultured in SCM1, SFM1, and SFM2 medium were subjected to chromosome G-banding analysis using Metafer (ZEISS). The hUC-MSCs were treated with colchicine (ST1173, Beyotime Biotechnology) for 4 h, followed by cell harvesting, treatment with hypotonic solution (0.075 mol/L KCl) for 30 min, and fixation. The fixed cells were dropped onto preheated slides, baked at 60 °C for 24 h, subjected to trypsin treatment, and stained with Giemsa (C0133, Beyotime Biotechnology).

#### In vitro tumorigenicity assay

P5 and P10 passages of hUC-MSCs cultured in the specified medium were utilized to evaluate the tumorigenicity. When cell confluency reached 80%, hUC-MSCs were mixed 1:1 with 0.7% agarose (VETEC-V900510, Sigma)

and seeded at a density of  $1 \times 10^4$  cells per well in 6-well plates previously embedded with 0.6% agarose. The cells were cultured for 4 weeks. After 4 weeks of culture, cells were washed with PBS and then fixed with 4% paraformaldehyde. Subsequently, cells were stained with 0.005% crystal violet (C0121, Beyotime Biotechnology) and washed with tap water until the agarose became transparent. H1299 and A5499 cells were used as positive control. The well without cells was used as blank control.

#### Secretory profile analysis of hUC-MSCs

To determine the secretory profile of hUC-MSCs, P4 and P9 hUC-MSCs were seeded at 6000 cells/cm<sup>2</sup> into 12-well plates and cultured in their respective media (SCM1, SCM2, SFM1, and SFM3) until reaching 80–90% confluence. After washing with PBS, the medium was removed and replaced with  $\alpha$ -MEM. After 36 h of culture, the supernatants from different hUC-MSCs groups were collected, centrifuged at 500 g for 10 min, and 1200 g for 10 min before being used for cytokines detection. The cytokine secretion profiles of hUC-MSCs were analyzed using the Bio-Plex Pro Human Cytokine Screening Panel (12007283, BIO-RAD). This assay measured 48 factors, including MIP-1 $\alpha$ , M-CSF, MIF, SCE, IL-17A, IL-7, IL-13, G-CSF, TRAIL, IL-4, MCP-3, Basic FGF, IL-5, LIF, MIG, IL-2, IL-2 $\alpha$ , IL-1R $\alpha$ , CTACK, IFN- $\alpha$ 2, IL-16, IL-18, PDGF-BB, VEGF, IL-15, TNF- $\alpha$ , IL-1 $\beta$ , IL-12p40, IL-12p70, IL-3, TNF- $\beta$ , HGF,  $\beta$ -NGF, IL-1 $\alpha$ , IL-10, SCGF- $\beta$ , IL-9, MIP-1 $\beta$ , RANTES, Eotaxin, SDF-1 $\alpha$ , IP-10, GM-CSF, IFN- $\gamma$ , IL-8, IL-6, GRO- $\alpha$  and MCP-1.

#### Cobblestone area forming cell (CAFC) assay

P5 and P10 hUC-MSCs cultured in SCM1, SCM2, SFM1, and SFM3 were used as feeder cells, and their support for HSC self-renewal was assessed by CAFC assays. The MS-5 murine fibroblast cell line was used as a control in the experiment [28]. P4 and P9 hUC-MSCs were seeded at 6000 cells/cm<sup>2</sup> into 24-well plates pretreated with 0.1% gelatin solution for 1 h and cultured in their respective medium until reaching 80–90% confluence. Once confluence was reached, the cells were irradiated with 20 Gy to inhibit cell growth. After irradiation, the cells were carefully washed and maintained in their respective medium for 2 days before being used as feeder cells for CAFC assays. 2000 CD34<sup>+</sup> HSC from UCB were resuspended in MyeloCult™ medium (05150, STEMCELL Technologies) with 350 ng/mL hydrocortisone (07925, STEMCELL Technologies) and seeded onto irradiated feeder cells in 24-well plates, with two wells per group, and incubated at 37 °C and 5% CO<sub>2</sub> for 14 days. Cultures were half-fed once a week, and CAFC were visualized using a phase-contrast microscope (ECLIPSE Ti2-E, NIKON CORPORATION) and counted if at least 5 cobblestone-like cells

were able to migrate beneath the feeder cells [28, 29]. At the end of the experiment, the total number of nucleated cells derived from UCB were assessed using trypan blue staining, and the proportion of CD34<sup>+</sup> cells was analyzed by flow cytometry.

**Detection of fungal and bacterial contamination**

The fungal and bacterial tests were conducted using the sterile examination method outlined in part 1101 of the 2020 edition of the Chinese Pharmacopoeia, and detections were performed using the detection kits (BZW12013 and BZW12012, Nanjing Lezhen Biotech) according to the manufacturer’s instructions.

**Measurement of endotoxin**

The endotoxin test was conducted using the method specified in part 1101 of the 2020 edition of the Chinese Pharmacopoeia, and detection was performed using Endotoxin Detection Kit (BK-T04, Zhangjiang Bokang Marine Biological) according to the manufacturer’s instructions.

**Virological testing**

P5 and P10 of hUC-MSCs were sent to Da’an gene located in Guangzhou for virological testing to evaluate the biosafety of the produced cells. Human immunodeficiency virus (HIV), cytomegalovirus (CMV), human hepatitis B virus (HBV), human hepatitis C virus (HCV), epstein–Barr virus (EBV), and human papilloma

virus (HPV) were detected by the methods described in Table 2.

**2.15 Statistical analysis**

All data are presented as the mean ± SEM of at least three independent experiments. The statistical significance of differences between groups was determined by Student’s t-test. Analyses and graphs were generated using Graph-Pad Prism version 8.0.2. For all statistical analyses, *P* < 0.05 indicated a statistically significant difference.

**Results**

**SCM can support cell growth while maintaining cellular biological characteristics**

To study the impacts of different types of culture media on hUC-MSCs biological characteristics, we first cultured cells in SCM, observed their morphology and activity across passages, and evaluated marker expression and differentiation potential at passages 5 and 10. Consistent with other research groups [30–32], cells cultured in medium containing 10% FBS exhibited spindle-shaped morphology (Fig. 1A). When expanded in SCM, the activity of hUC-MSCs is maintained between 85% and 95%, and the PDT is maintained between 25 h and 32 h (Fig. 1B). Flow cytometry analysis revealed that hUC-MSCs at passages 5 and 10 showed high expression (≥ 95%) of CD73, CD90, and CD105, while lacked expression (≤ 2%) of CD34, CD45, CD14, CD19, and HLA-DR surface molecules, which is consistent with the definition of MSCs by ISCT (Fig. 1C). Induction differentiation of

**Table 2** Safety standards of hUC-MSC

Safety standards of hUC-MSC			
Items	Methods	Quality standards	Results
Human immunodeficiency virus (HIV) qualitative detection	Nested PCR fluorescence method	Negative	Negative
Human immunodeficiency virus (HIV) quantitative detection	Nested PCR fluorescence method	< 100 IU/mL	< 100 IU/mL
Cytomegalovirus (CMV) qualitative detection	PCR	Negative	Negative
Cytomegalovirus (CMV) quantitative detection	FQ-PCR	< 500 copies/mL	< 500 copies/mL
Human hepatitis B virus (HBV) qualitative detection	PCR	Negative	Negative
Human hepatitis B virus (HBV) quantitative detection	FQ-PCR	< 100 IU/mL	< 100 IU/mL
Human hepatitis C virus (HCV) qualitative detection	PCR	Negative	Negative
Human hepatitis C virus (HCV) quantitative detection	FQ-PCR	<50 IU/mL	< 50 IU/mL
Epstein-Barr virus (EBV) qualitative detection	PCR	Negative	Negative
Epstein-Barr virus (EBV) quantitative detection	FQ-PCR	< 500 copies/mL	< 500 copies/mL
Human papilloma virus (HPV) quantitative detection	FQ-PCR	< 500 copies/mL	<500 copies/mL
Endotoxin test	Endpoint colorimetric assay	< 0.25 EU/mL	< 0.25 EU/mL
Mycoplasma detection	Culture method	Negative	Negative
Sterility testing	Culture method	Negative	Negative
Karyotype analysis	G-band method	46XX or 46XY	46XX or 46XY
Tumorigenicity test	Soft agar clone formation experiment	Negative	Negative

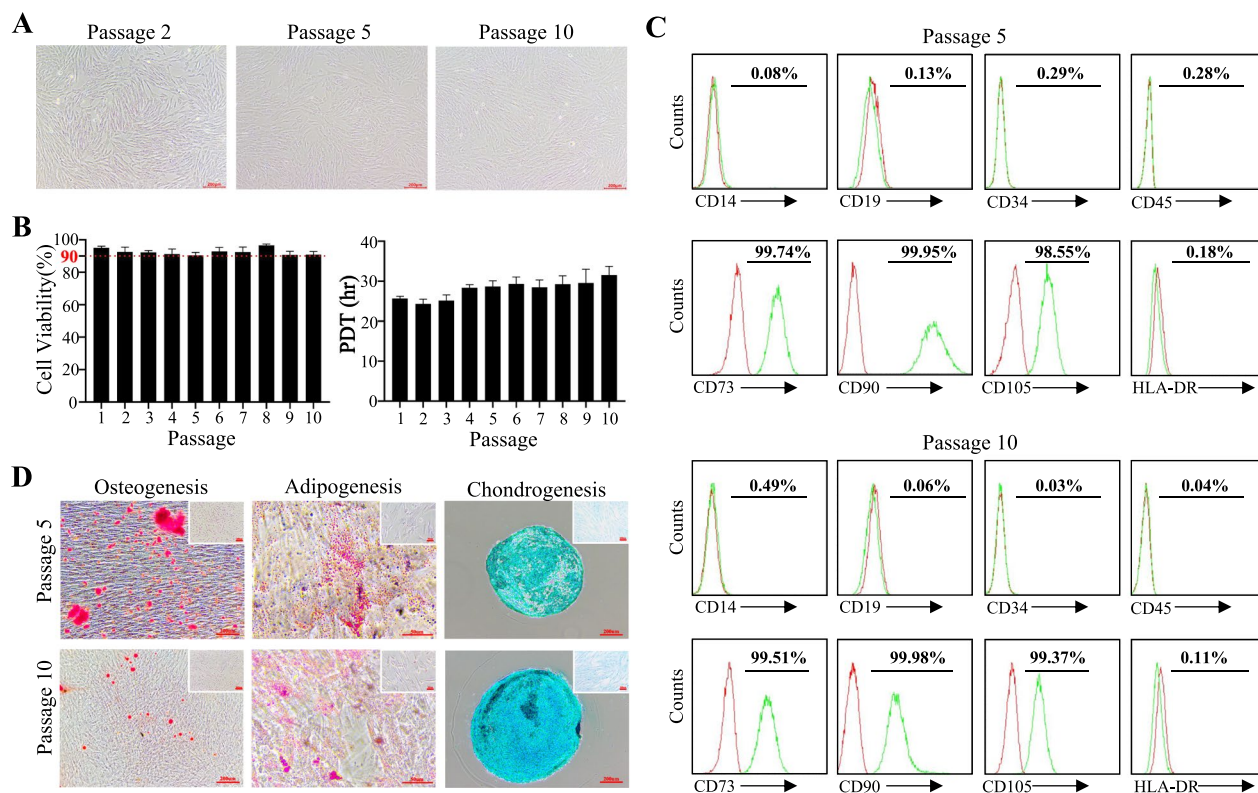


**Fig. 1** SCM support hUC-MSCs while maintaining cellular characteristics. hUC-MSCs were cultured in SCM to indicated passages. **A** Cell morphology was assessed by optical microscopy. **B** Cell viability and PDT were assessed at different passages. **C** Levels of indicated surface markers of hUC-MSCs from P5 and P10 were determined by FACS. **D** The differentiation potential of hUC-MSCs into three lineages were assessed at P5 and P10. hUC-MSCs cultured without osteogenic, chondrogenic, or adipogenic differentiation stimuli were used as negative control and shown in the figure inserts. Results shown in B are expressed as means  $\pm$  SEM. Data shown in A-D are representative of at least three separate experiments.

hUC-MSCs at passages 5 and 10 revealed that cells have the potential to differentiate into osteogenic, adipogenic, and chondrogenic lineages (Fig. 1D).

#### SFM effectively support the serial passaging of hUC-MSCs while maintaining their biological characteristics from passages 2 to 10

Due to the xenogeneic components in FBS, hUC-MSCs cultured in SCM pose potential risks of contamination and immune reactions when used for clinical treatment of diseases [24]. To address this, we developed a formulation of SFM (SFM1) using platelet lysate and other additives as a substitute for animal serum and evaluated the impacts of SFM1 on cell phenotype and function (Table 1). We found that hUC-MSCs cultured in SFM1 exhibited consistent cellular morphology, surface molecules expression, and differentiation potential with the criteria defined by ISCT (Fig. 2A-2D). hUC-MSCs cultured in SFM1 exhibited a spindle-shaped growth pattern from passages 2 to 10 (Fig. 2A). When expanded in SFM1, the activity of hUC-MSCs is maintained between 90% and 98%, and the PDT is maintained between 20 h

and 27 h (Fig. 2B). Flow cytometry analysis revealed that hUC-MSCs at passages 5 and 10 showed high expression ( $\geq 95\%$ ) of CD73, CD90, and CD105, while lacked expression ( $\leq 2\%$ ) of CD34, CD45, CD14, CD19, and HLA-DR surface molecules (Fig. 2C). hUC-MSCs at passages 5 and 10 have the potential to differentiate into osteogenic, adipogenic, and chondrogenic lineages (Fig. 2D).

#### SFM offer greater benefits for clinical-grade industrial-scale production of hUC-MSCs compared to SCM

For large-scale production of clinical-grade hUC-MSCs, it is necessary to optimize cell manufacturing processes to meet the demands of industrial-scale cell production for inter-batch consistency, cost-effectiveness, passage stability, biological safety, and efficacy. Maximizing the yield of hUC-MSCs within a given timeframe or obtaining a greater quantity of highly active hUC-MSCs at comparable costs is a central goal in optimizing cell production processes. This endeavor will empower producers in the field of cell therapy to gain a substantial competitive advantages.

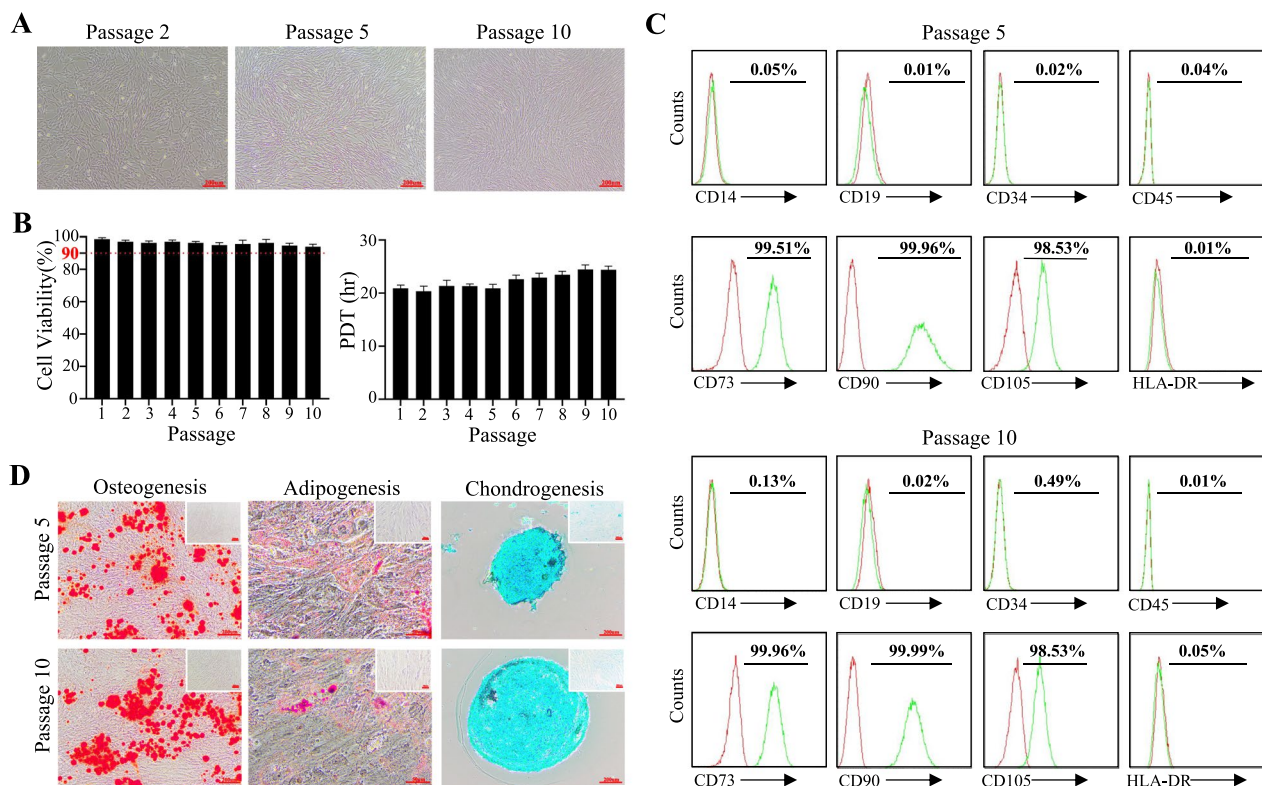


**Fig. 2** SFM1 support hUC-MSCs while maintaining cellular characteristics. hUC-MSCs were cultured in SFM1 to indicated passages. **A** Cell morphology was assessed by optical microscopy. **B** Cell viability and PDT were assessed at different passages. **C** Levels of indicated surface markers of hUC-MSCs from P5 and P10 were determined by FACS. **D** The differentiation potential of hUC-MSCs into three lineages were assessed at P5 and P10. hUC-MSCs cultured without osteogenic, chondrogenic, or adipogenic differentiation stimuli were used as negative control and shown in the figure inserts. Results shown in B are expressed as means  $\pm$  SEM. Data shown in A-D are representative of at least three separate experiments.

We developed SFM1 and compared the differences among SFM1 and two SCM (SCM1 and SCM2) in terms of cell viability, multiple increase, cell doubling time, and cellular senescence from passage 2 to passage 10. We found that using 5% platelet lysate in SFM1 yielded higher quantity hUC-MSCs compared to two SCM requiring 10% FBS, providing a cost advantage (Fig. 3A). More importantly, by comparing the activity differences between cells cultured in SFM1 and two SCM across different passages, we discovered that cells cultured in SFM1 exhibited higher activity than those in two SCM (Fig. 3B). In terms of cell passage stability, we observed that although the cell viability gradually decreased with increasing passages in both SFM1 and two SCM, SFM1-cultured cells exhibited smaller fluctuations in cell activity between different passages, indicating higher stability compared to two SCM cultivation (Fig. 3B). Consistently, SFM1-cultured cells exhibited shorter PDT and smaller variations in doubling time between different passages (Fig. 3C).

Furthermore, we conducted  $\beta$ -galactosidase staining experiments to compare the cellular senescence

between SFM1 and two SCM cultured cells at different passages. The results revealed that SFM1-cultured cells exhibited slower rates of cellular senescence (Fig. 3D). Interestingly, we found that while cells cultured in both SFM1 and two SCM exhibited tri-lineage differentiation potential, alizarin red staining experiments indicated that cells cultured in SFM1 displayed superior osteogenic differentiation potential at passage 10 compared to two SCM groups (Fig. 3E). These results suggested that utilizing customized SFM1 for cell culture enables the production of a higher quantity of cells with better activity and quality within the same timeframe, which highlights the greater potential value of SFM in producing clinical-grade hUC-MSCs. Considering the differences in osteogenic differentiation potential between cells cultured in SFM1 and two SCM, it is important to optimize the culture media formulation based on the specific disease being treated in order to achieve the best therapeutic outcomes.

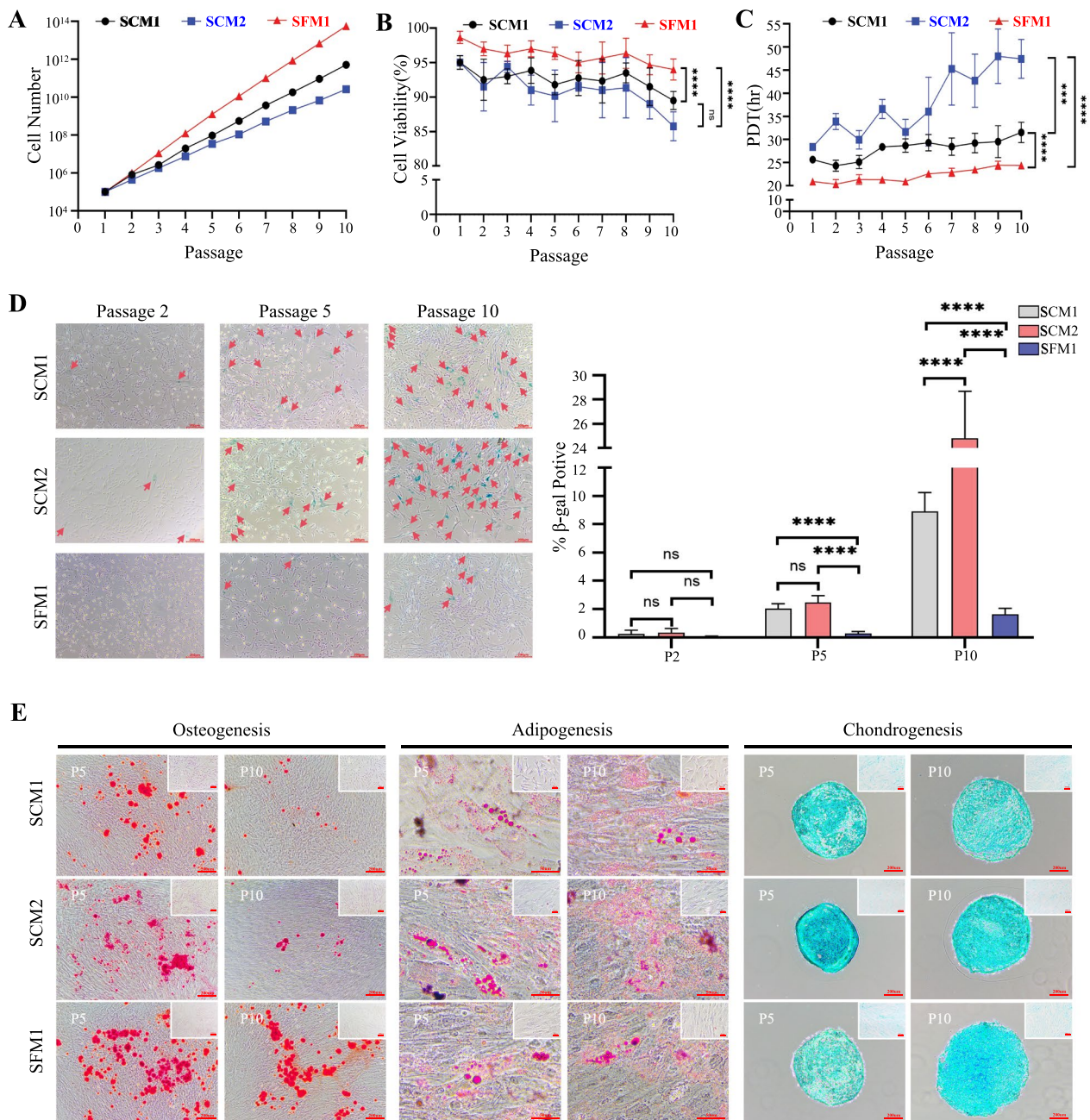


**Fig. 3** SFM1 offer greater benefits for clinical-grade industrial-scale hUC-MSCs production compared to SCM. hUC-MSCs were cultured in SFM1 and two SCM to corresponding passages. **A-C** Cell number, cell viability, and PDT were assessed using at indicated passages. **D** The senescence status of hUC-MSCs was assessed and analyzed by using β-galactosidase staining. The β-gal-positive cells are indicated by the red arrows. **E** The differentiation potential of SFM1 and two SCM cultured hUC-MSCs into three lineages were assessed at P5 and P10. hUC-MSCs cultured without osteogenic, chondrogenic, or adipogenic differentiation stimuli were used as negative control and shown in the figure inserts. Results shown in B-D are expressed as means ± SEM. Data shown in A-E are representative of at least three separate experiments. \*\*\**p* < 0.001; \*\*\*\**p* < 0.0001.

**The phenotype and biosafety detection of hUC-MSCs cultured in different SFM**

Subsequently, we developed four different formulations of hUC-MSCs and investigated the effects of these

media on cell phenotype and biosafety. Under the optical microscope, hUC-MSCs exhibited spindle-shaped morphology in all four media, with cells cultured in SFM1 showing a more slender shape compared to those in

SFM2, SFM3 and SFM4 (Fig. 4A). Consistent with this, when evaluating the differences between hUC-MSCs cultured in different media using the ratio of cell length to width (L: W), hUC-MSCs cultured in SFM1 were significantly better than those cultured in SCM and other SFM (Fig. 4B). Surface molecular identification confirmed that hUC-MSCs cultured in all four SFM are MSCs, and they exhibited multilineage differentiation potential at both P5 and P10 (Fig. 4C and D). Quantitative analysis of differentiated cells revealed that hUC-MSCs cultured in SFM1 exhibited significantly enhanced osteogenic differentiation at passage 10 compared to those in SFM2, SFM3, and SFM4 (Fig. 4C). The endotoxin and sterility tests conducted on hUC-MSCs cultured in the four SFM all yielded negative results (Table 2). Virological testing conducted on hUC-MSCs cultured in SFM at passages 5 and 10 revealed no viral contamination (Table 2). Soft agar cloning experiments revealed that hUC-MSCs cultured in all SFM at passages 5 and 10 did not form colonies, while positive control H1299 and A549 cells did, indicating that hUC-MSCs cultured in these SFM have no tumorigenic risk (Fig. 4E and Supplementary Fig. S1). These results suggested that the phenotype and biosafety of all the SFM cultured hUC-MSCs meet the requirements of cell therapy industry. Additionally, SFM1 outperforms other media in terms of cell morphology and osteogenic differentiation capacity, indicating that SFM1 holds greater commercial application potential in the future.

#### The phenotype and function of hUC-MSCs differ depending on the different SFM

To further investigate the differences in phenotype and function of hUC-MSCs cultured in various SFM and SCM, we cultured hUC-MSCs with identical cell seeding densities in different SFM and SCM until passage 10 and examined the changes in cell viability, proliferation rates, and senescence levels. We found that the cell viabilities maintained at 90%~98% across the four SFM, with SFM1 exhibiting a higher average level than other SFM and SCM groups (Fig. 5A). Additionally, the PDT of SFM1 cultured hUC-MSCs was significantly lower than other SFM and SCM (Fig. 5B). Despite the proportion of senescent cells gradually increased with passages in all culture media, SFM1 cultured hUC-MSCs exhibited the lowest

proportion of senescent cells (Fig. 5C and Supplementary Fig. S2). By analyzing and comparing the proliferation curves of cells at passages 5 and 10, we found that hUC-MSC in SFM1 exhibited better PPL than others (Supplementary Fig. S3 and Fig. 5D). Consistently, the analysis of the cell cycle in P5 and P10 generations reveals that the proportions of S and G2/M stages of hUC-MSCs cultured in SFM1 were higher than other groups (Supplementary Fig. S4 and Fig. 5E). Chromosome karyotype analysis revealed no chromosomal aberrations in hUC-MSCs cultured in SCM1, SFM1 and SFM2 at passages 5 and 10 (Fig. 5F). We also observed that cells cultured in SCM1 medium required prolonged treatment with enzyme trypsin during passage compared to other culture media (Fig. 5G).

Considering that the paracrine function is one of the main mechanisms of therapeutic action of MSCs, we used liquid chip technology to further assess the cytokines profiles released by P5 and P10 hUC-MSCs cultured in different media (SCM1, SCM2, SFM1 and SFM3). From the results of the heat map (Fig. 6A), we found that the cytokine secretion profile of SCM2 cultured hUC-MSCs exhibited lower similarity to the other groups, which was consistent with the differences in cell proliferation capacity and cell senescent rates across the groups. Interestingly, we found that among the eight sample groups, hUC-MSCs cultured in SFM1 showed the greatest similarity in cytokine secretion profiles between P5 and P10, with most cytokines being highly expressed, whereas the other groups did not exhibit this pattern. This indicated that the medium plays a significant role in supporting the long-term maintenance of cytokine secretion by the cells (Fig. 6A). After investigating and analyzing the role of each factor in detail, we categorized the cytokine profiles into five major groups: angiogenesis, pro-inflammatory (Pro-), anti-inflammatory (Anti-), recruitment and multi-function (Multi-) (Fig. 6B and C). Comparative analysis revealed that at P5 stage, the SFM1 and SCM1 groups showed greater similarity and the highest levels of secreted factors, while at P10 stage, the SFM1 and SFM3 groups displayed more similarity and had the highest levels of secreted factors.

Many studies have reported that MSCs play a significant role in promoting the recovery of hematopoietic

(See figure on next page.)

**Fig. 4** The phenotype and biosafety detection of hUC-MSCs cultured in different SFM. hUC-MSCs were cultured in different SFM and SCM to corresponding passages. **A** Cell morphology was assessed by optical microscopy, and **B** analyzed by the aspect ratio of cell length to width (L: W). **C** The differentiation potential of customized different SFM cultured hUC-MSCs into three lineages were assessed at P5 and P10. **D** Levels of indicated surface markers of hUC-MSCs from P5 and P10 were determined by FACS. **E** P5 and P10 passages of hUC-MSCs cultured in different customized SFM were utilized to evaluate the tumorigenicity. Results shown in B and D are expressed as means  $\pm$  SEM. Data shown in A-E are representative of at least three separate experiments. \* $p < 0.05$ ; \*\* $p < 0.01$ ; \*\*\* $p < 0.001$ ; \*\*\*\* $p < 0.0001$ .

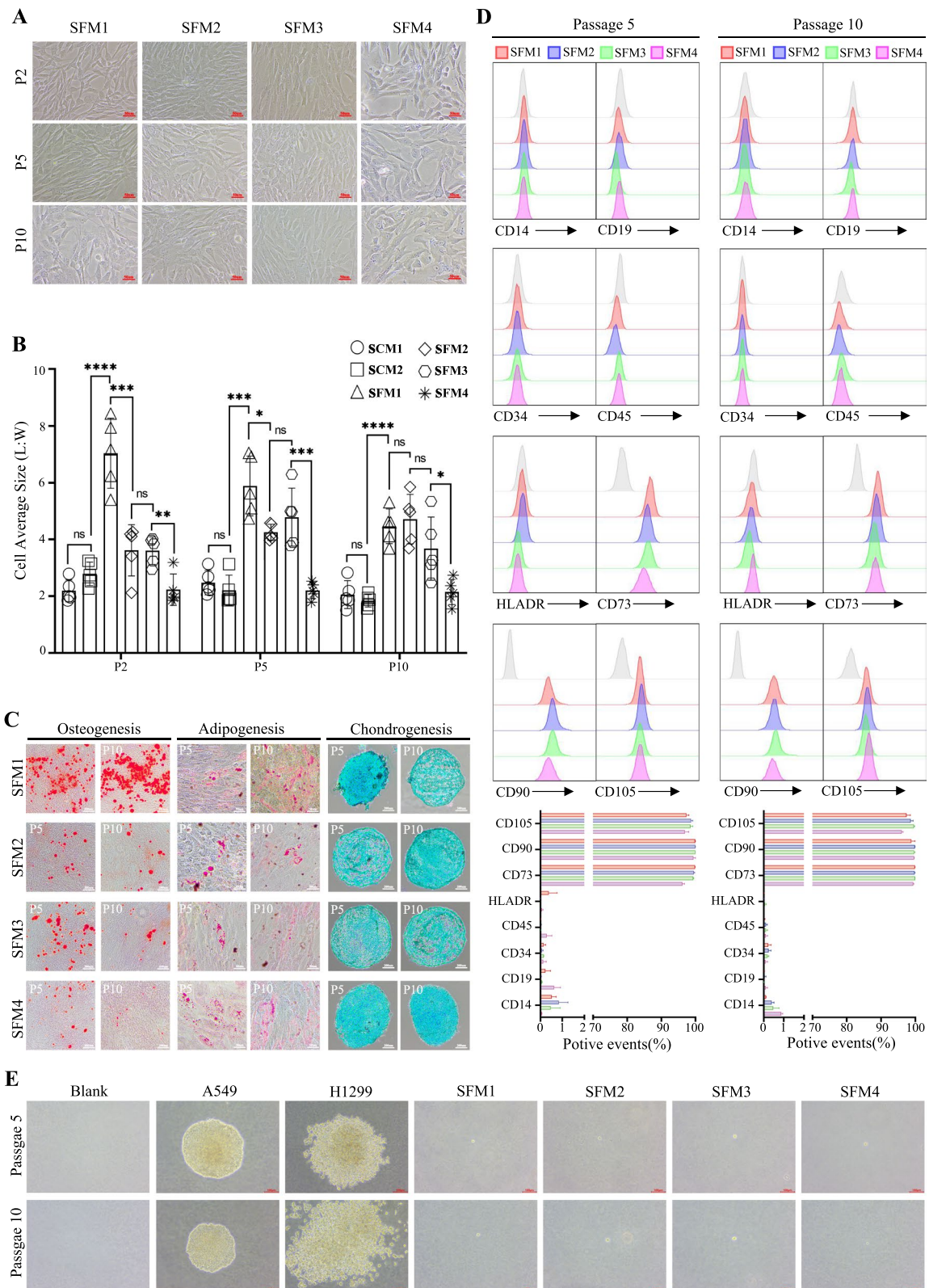


**Fig. 4** (See legend on previous page.)

function [33–35]. When MSCs are infused together with HSC, they can markedly accelerate the restoration of hematopoietic function in patients, with safety and fewer adverse reactions. We used CAFC assay to assess whether there are differences in the hematopoietic function and self-renewal ability of HSC cultured with different feeder cells [28]. At day 14, we found that a CD34+ cell population was maintained in the culture, with a proportion ranging from 18.89 to 52.68% (Fig. 7A and B). Regarding this CD34+ cell population, differences were observed when hUC-MSCs cultured in different media were used as feeder layers, regardless of whether P5 or P10 cells were used. Counting and analysis of cobblestone-like cells revealed that hUC-MSCs, regardless of the culture medium, all of them allowed the formation of CAFC by UCB derived HSC (Fig. 7C and D). After 14 days of co-culture with different groups of hUC-MSCs, the number of HSC increased by 39.8 to 110.7 times compared to the initial seeding number, which is higher than the control group (MS-5) (Fig. 7E). Additionally, we observed that UCB cells expanded more on P6 cells than on P9 cells, regardless of the culture media used for the feeder cells (Fig. 7F). Moreover, we found that when hUC-MSCs cultured in SFM1 were used as feeder cells, UCB cells maintained the highest proportion of the CD34+ population and achieved higher expansion fold (Fig. 7B and E), but formed the lowest number of CAFC (Fig. 7C).

We simultaneously compared the changes of hUC-MSCs in cell viability, multiple increase and PDT after cryopreservation and revival in SFM and SCM. The results demonstrated that cryopreservation and subsequent revival procedures resulted in decreased cell viability and expansion fold, along with extended PDT in both P5 and P10 generations of cells, with a more pronounced impact observed in P10 generation cells compared to P5 generation cells (Supplementary Fig. S5A–E). Although cell viability gradually recovered after 1–2 passages, the extent of recovery was associated with the pre-freeze cell state and the culture medium used. We observed that the post-thaw recovery process led to increased PDT and decreased expansion fold for cells cultured in different media, cells cultured in SFM1 gradually recovered to pre-cryopreservation levels after 1–2 passages (Supplementary Fig. S5C).

The above results further demonstrate that although different culture media can cultivate MSCs that fulfill the ISCT definition based on cell morphology, surface molecules expression, and trilineage differentiation potential, MSCs cultured in different media exhibit differences in cell viability, proliferation time, trilineage differentiation potential, senescence rate, population expansion capacity, paracrine function, and support for HSC self-renewal. These results suggested that during large-scale production of clinical-grade hUC-MSCs, SFM offer several advantages over SCM in terms of batch-to-batch consistency, cost-effectiveness, passage stability, and biological safety. Considering the differences in cell morphology, senescence rate, differentiation potential, paracrine function and support for HSC self-renewal of hUC-MSCs cultured in different SFM and SCM, the choice of culture media may indeed play a critical role in determining whether hUC-MSCs can achieve optimal therapeutic effects in future commercial applications and disease treatments.

## Discussion

Currently, preclinical studies have found that hUC-MSCs may be explored in various challenging and serious diseases such as diabetes, liver failure, systemic lupus erythematosus, and osteoarthritis [36–40]. The cell culture medium is the key material in cell production, determining the fundamental functions of the cells [12, 41]. Traditional expansion of MSCs using medium containing FBS increases the clinical application risks [24, 42]. Using SFM to produce clinical-grade hUC-MSCs is becoming the prevailing trend in industrial development [27, 43, 44].

Other groups have previously reported that different components in culture media promote MSCs proliferation [45–49]. These studies mainly focused on whether different formulations of media could cultivate MSCs that meet the standards in terms of cell morphology, surface molecular markers, and trilinear differentiation potential. However, there is limited research conducted from the perspective of cell therapy industry to assess whether cells cultured in different formulations of media meet the requirements of industrial-scale cell production. The commercial application of cell therapy is largely determined by whether the cultured cells can meet the

(See figure on next page.)

**Fig. 5** The effects of customized SFM on the phenotype and function of hUC-MSCs. hUC-MSCs were cultured in SFM and SCM to corresponding passages. **A, B** Cell viability and PDT were assessed at different passages. **C** The senescence status of hUC-MSCs was assessed and analyzed by using  $\beta$ -galactosidase staining. **D** The PPL and **E** cell cycle of hUC-MSCs were determined at passages 5 and 10. **F** Chromosome karyotype of hUC-MSCs were analyzed at indicated passages. **G** Comparison of cell digestion time in customized media. Results shown in A–E are expressed as means  $\pm$  SEM. Data shown in A–G are representative of at least three separate experiments. \* $p < 0.05$ ; \*\* $p < 0.01$ ; \*\*\* $p < 0.001$ ; \*\*\*\* $p < 0.0001$ .

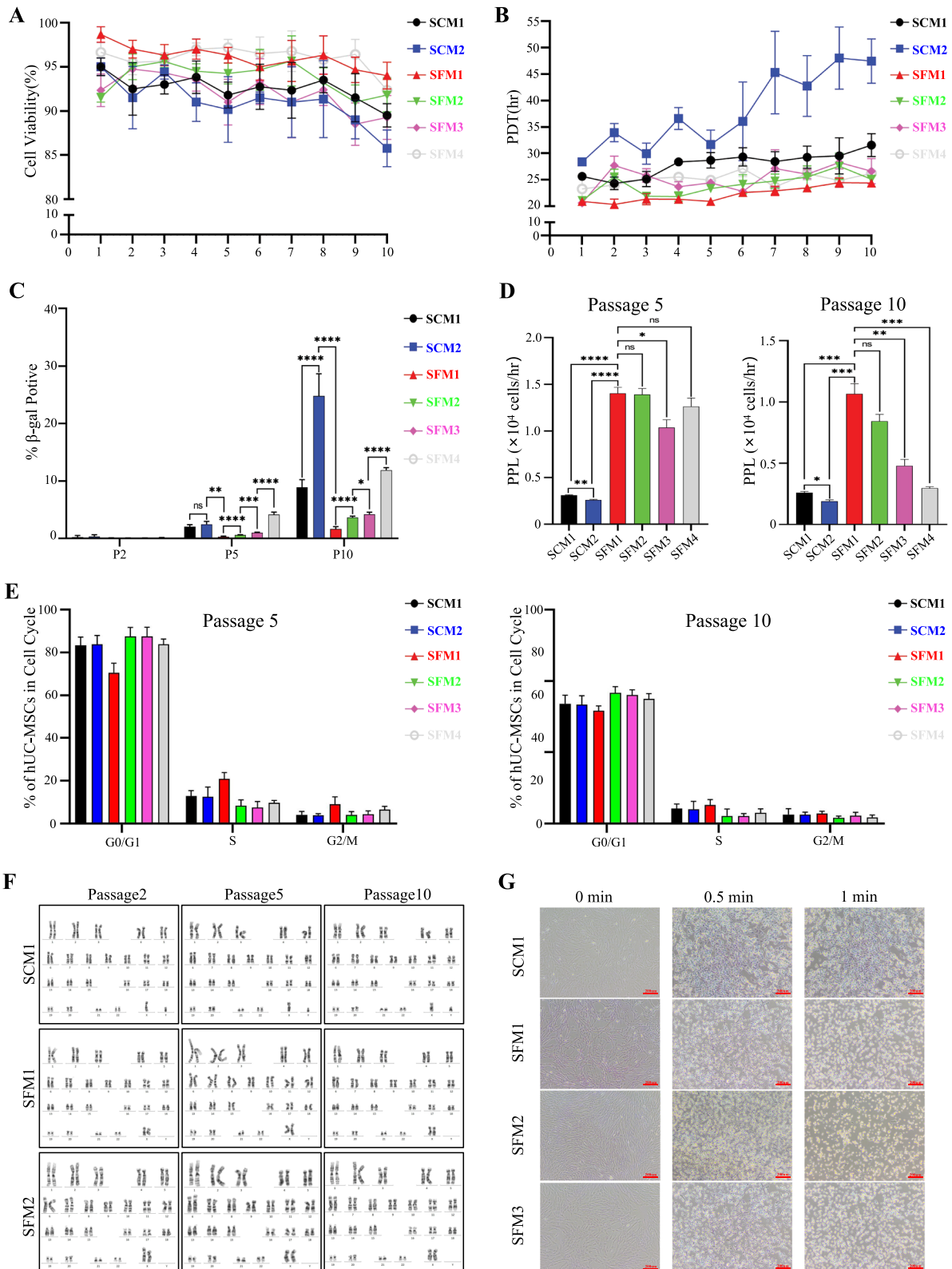


**Fig. 5** (See legend on previous page.)

requirements of inter-batch consistency, efficacy, stability, biosafety, and cost-effectiveness. Therefore, we developed a series of SFM and SCM to elucidate the effects of different media on hUC-MSCs phenotype and function. By comparing and analyzing the commercial application requirements of the cell therapy industry with the effects of the different culture media on cell phenotype and function, our results demonstrated that customized culture media significantly impact the inter-batch consistency, efficacy, stability, biosafety, and cost-effectiveness required for industrial-scale cell production.

Considering that cultured MSCs will be applied in clinical disease therapy rather than scientific research, media containing FBS are restricted due to the presence of xenogeneic compositions. Consistent with many studies [50–52], our study found that replacing FBS with platelet lysate to develop SFM resulted in better effects on cell phenotype and function compared to SCM indicating that platelet lysate is one of the best alternatives to FBS. It is noteworthy that hUC-MSCs cultured in SFM2, SFM3, and SFM4 exhibited differences in cell viability, PDT, and cellular senescence rate, indicating that different brands of platelet lysates used in SFM could have distinct effects on cell phenotype and function. Additionally, many studies have demonstrated that different factors have varying effects on cell growth and function [53–56]. In this study, comparing the effects of SFM1 and SFM2 on hUC-MSCs phenotype and function revealed that additives play a crucial role in shaping cell phenotype and function. These results suggested that establishing a customized SFM research platform is highly valuable for cell production companies to accelerate the commercial application of cell-based therapies.

The method for preparing SFM that we have developed could serve as a platform for the clinical-grade production of UC-MSCs in the future. By incorporating human platelet lysate and other additives to completely replace xenogeneic serum, a range of SFM can be obtained to generate therapeutic hUC-MSCs tailored for optimal efficacy in specific diseases. Interestingly, through comparative analysis of the formulations among different SFM and their respective impacts on cellular phenotype and function, we observed significant influences from the basal culture medium, human platelet lysate, and other additives. This underscores their collective role in

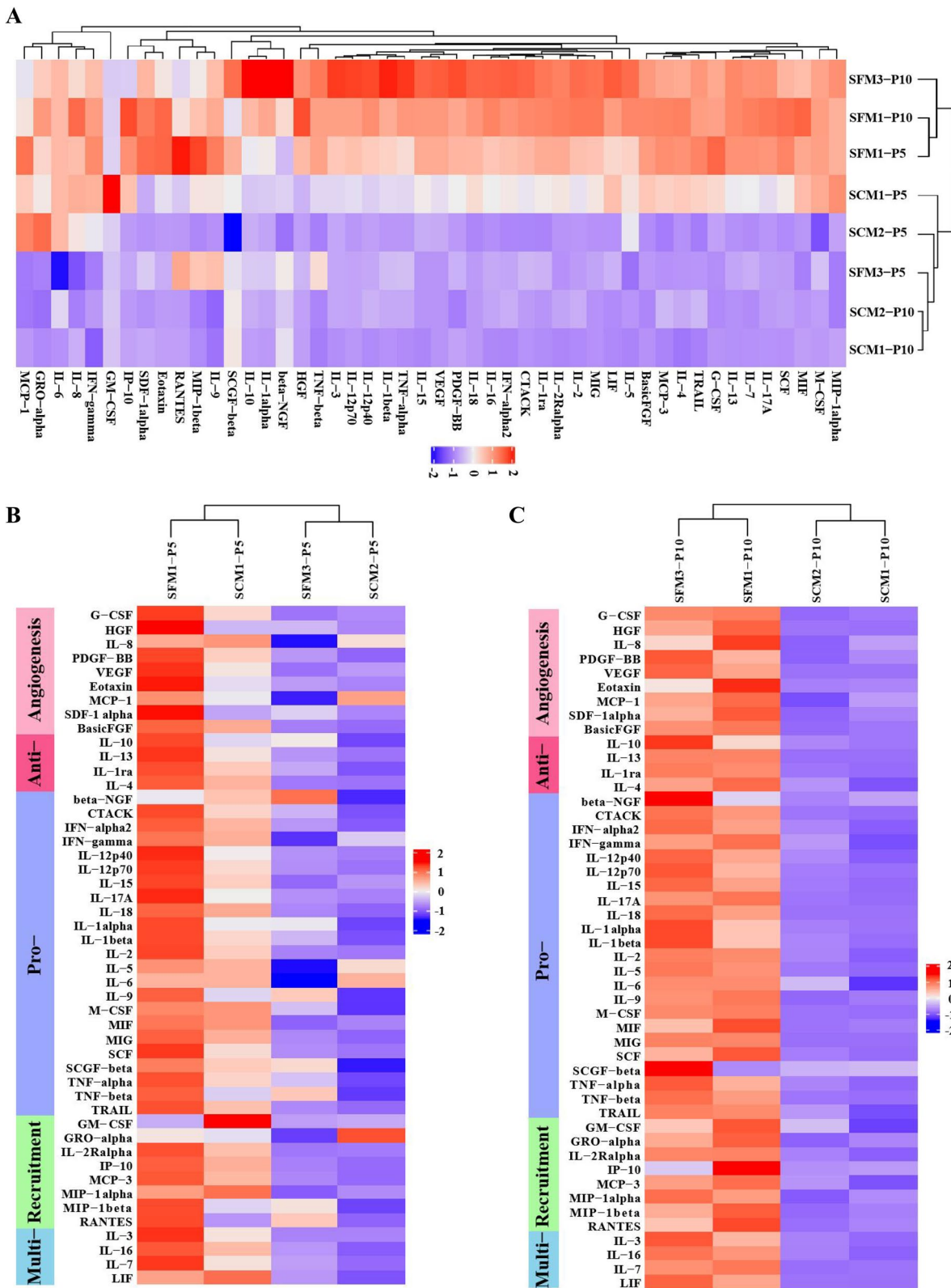
shaping cellular characteristics and functionalities. These results underscore the necessity for comprehensive optimization of culture media components specific to each disease prior to conducting clinical trials of cell-based therapies.

A substantial amount of MSCs resources is required when utilized for disease treatment [57, 58]. To obtain cost-effective clinical-grade hUC-MSCs, it is essential to optimize the entire production process to yield a greater quantity of high-quality cells within the same timeframe. In this study, we developed a platform to create series of SFM by substituting serum with platelet lysate and other additives, which are cost-equivalent or even lower priced than SCM. hUC-MSCs cultured in the four formulations of SFM were successfully expanded up to the 10th passage, indicating that the SFM obtained through this platform effectively supports cell growth. The cost of culturing cells using SFM is comparable to SCM, but the yield of hUC-MSCs cultured in SFM1 is more than 100 times higher than that in SCM after ten passages. Therefore, cost-benefit analysis reveals that our laboratory-developed SFM formulation platform supports a transition from SCM to SFM for cell culture. The various SFM formulations in this study demonstrate superior or comparable support for cell growth compared to SCM, indicating that the approach of formulating SFM in this research can lead to the development of a broader range of SFM formulations. This provides a specific technical method for optimizing production processes in the future, ultimately enabling the production of more cost-effective clinical-grade hUC-MSCs.

Several studies have reported functional differences among MSCs sourced from different tissues, highlighting potential variations in clinical applications [59–63]. The selection of MSCs from different tissue sources for the same disease may result in differences in therapeutic efficacy. However, there is a lack of research investigating whether cells cultured in different media formulations exhibit differences in therapeutic efficacy for diseases. Although many studies, including our own, have found that SFM can provide adequate nutrients to generate MSC meeting ISCT standards [22, 64–67], these studies lack systematic studies on the differences in phenotype and function of cells cultured in different media. All these differentiated functions in

(See figure on next page.)

**Fig. 6** The cytokine secretion profiles of hUC-MSCs cultured with different types and compositions of culture media. The culture supernatants of P5 and P10 hUC-MSCs cultured with SFM and SCM were used for liquid chip analysis. **A** Heatmap analysis of the similarity in cytokine secretion profiles among different groups of hUC-MSCs. **B–C** Comparative analysis of the pattern changes in 48 cytokines between P5 and P10 hUC-MSCs across different groups. The data from the liquid chip are normalized to standard normal distribution. The scale represent the expression values of the factors after standardization (the redder the color, the higher the expression value; the bluer the color, the lower the expression value).



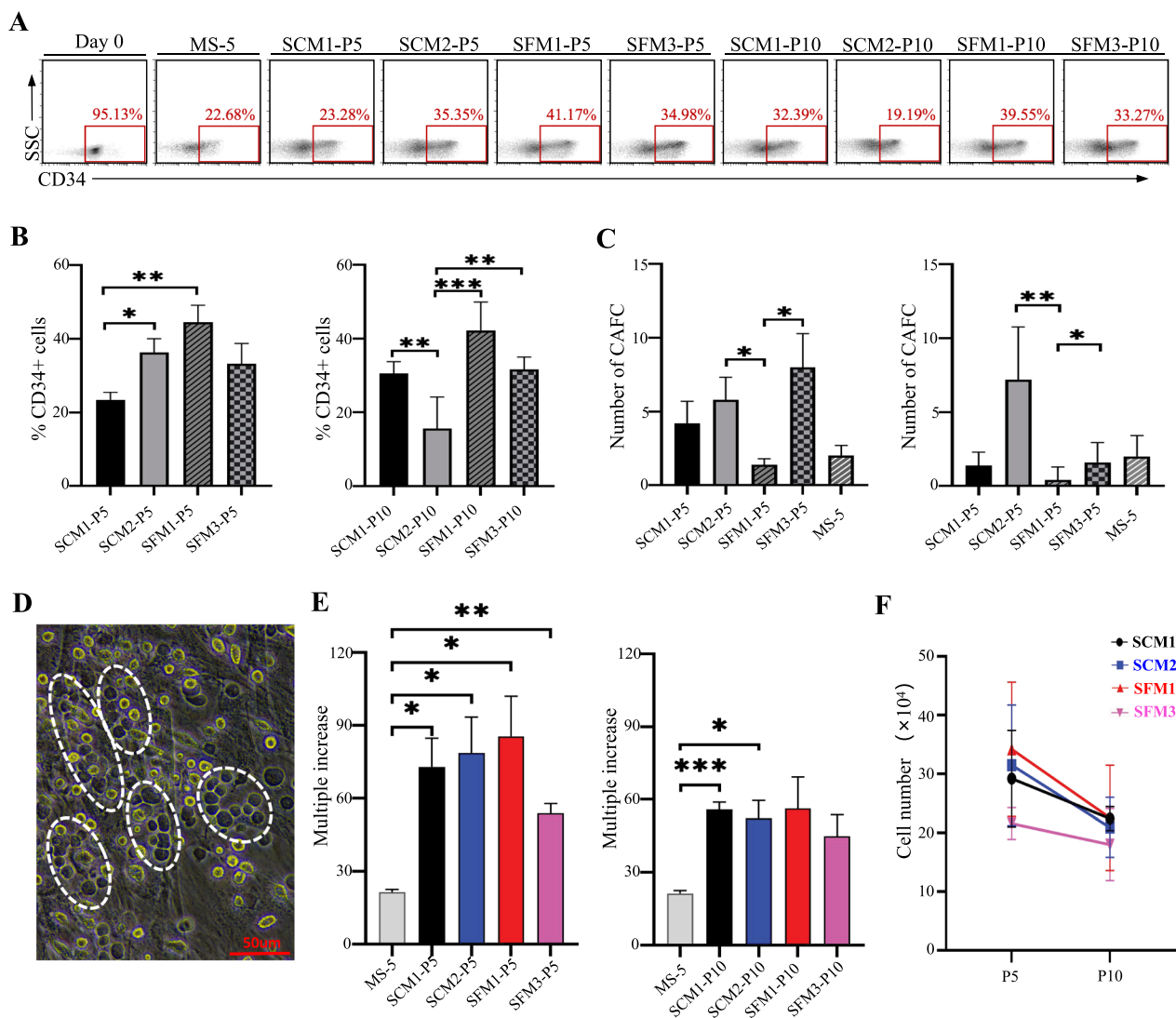


**Fig. 7** The impact of hUC-MSCs cultured with different media on the self-renewal and CAFC formation abilities of HSC. P5 and P10 hUC-MSCs cultured with SFM and SCM were used as feeder cells for CAFC assays. **A** The representative images of the expression of CD34 on UCB cells before and after co-culture with feeder cells. **B** Statistical diagram of the proportion of CD34+ UCB cells after 14 days of co-culture with feeder cells. **C** Analysis of CAFC numbers after 14 days of co-culture between UCB cells and feeder cells. **D** The representative image of CAFC. The cobblestone areas are indicated by the white circles. **E** The expansion fold of UCB cells after co-culture with feeder cells for 14 days. **F** Comparative analysis of the impact of P5 and P10 feeder layer cells on the expansion of UCB cells. Results shown in B, C, E and F are expressed as means ± SEM. Data shown in A-F are representative of at least three separate experiments. \**p* < 0.05; \*\**p* < 0.01; \*\*\**p* < 0.001

hUC-MSCs could play a crucial role in the efficacy of subsequent disease treatments, thus warranting careful consideration. To our knowledge, this is the first study aimed at industrial-scale production of clinical-grade hUC-MSCs, evaluating the impact of various SFM and SCM on the phenotype and function of hUC-MSCs, thus exploring the importance of media selection for the commercial application of cell therapy industry. The differences observed in various biological indicators among hUC-MSCs cultured in different SFM pose

greater challenges in selecting the appropriate media for producing clinical-grade hUC-MSCs.

Liquid chip analysis revealed substantial differences in factors secreted by hUC-MSCs cultured in different media, indicating a close relationship between cell function and the selected culture medium. Additionally, the significant differences in cytokine secretion between different passages of cells produced in the same medium suggest that when developing cell-based therapeutics, the choice of medium must be carefully integrated with the

overall stem cell production process. Further research is needed to determine whether using cells of different passages for new drug development affects clinical treatment outcomes.

The ability of hUC-MSCs to promote HSC self-renewal suggested that hUC-MSCs could play a positive role in clinical HSC transplantation therapies. In the experiment, we observed that hUC-MSCs cultured in SFM1 as feeder cells resulted in the highest proportion of CD34+ UCB cells and higher expansion, yet the lowest number of CAFs. This suggested that hUC-MSCs in SFM1 are more conducive to UCB cell proliferation rather than CAFs formation. The differences in the ability of MSCs cultured in different media to support HSC proliferation and CAFs formation suggested that careful selection of culture medium is crucial when producing MSCs for clinical use in HSC transplantation, as certain medium may yield MSCs that better maintain the original state of HSC and promote their expansion, thereby enhancing transplantation success and long-term hematopoietic reconstitution. The differences in support for HSC self-renewal between P5 and P10 hUC-MSCs further underscored the importance of optimizing stem cell production processes in clinical disease treatments. However, more research is needed to determine the impact of production processes on the efficacy of cell-based therapies.

Our results suggested that for the production of hUC-MSCs intended for clinical therapy, media selection should not only focus on whether the media can cultivate MSCs meeting minimum standards by cell morphology, surface molecules and trilineage differentiation potential. Rather, it is crucial to prioritize selecting the appropriate media based on the future intended use of the MSCs through systematic research, aiming to optimize the efficacy of the cells for specific disease treatments.

Compared to cells cultured in SCM and other SFM, hUC-MSCs in SFM1 maintain basic biological characteristics after long-term *in vitro* culture, exhibiting a thinner, smaller morphology and size, slower aging rate and superior osteogenic differentiation and proliferation capabilities. These findings are consistent with those of some research groups but differ from others, which may be attributed to variations in the growth factors added to the media by different research groups [46, 68–71]. These results suggested that compared to SCM, hUC-MSCs cultured through SFM exhibit higher stability across different generations.

In this study, hUC-MSCs cultured in SFM at passages 5 and 10 exhibited high expression levels of CD73, CD90, and CD105 ( $\geq 95\%$ ), along with low expression levels of CD34, CD45, CD14, CD19, and HLA-DR ( $\leq 2\%$ ), indicating that hUC-MSC cultured with SFM can meet the minimum key markers defined by ISCT

in high generations. The cell activity and PDT of hUC-MSC cultured in SFM were significantly better than those cultured in SCM at higher passages, indicating that the stability between passages of hUC-MSC cultured in SFM was higher than that of cells cultured in SCM, further demonstrate that the quality of SFM cultured cells is better.

We found that cryopreservation and subsequent revival procedures will lead to a decreased post-revival viability, proliferation, and increased doubling time in both P5 and P10 generations of cells, which suggested that cryopreservation and revival processes have a significant impact on the development of cellular drugs. We also observed that despite the reduction in cell doubling time upon revival following cryopreservation, cells cultured in SFM1 gradually recover to pre-cryopreservation levels after 1–2 passages. All these results indicate that the development of cell drugs cannot be achieved without the support of high-quality culture media and cryopreservation solutions.

Biological safety assessment is one of the primary concerns in industrial hUC-MSCs production, particularly for cells cultured long-term *in vitro*, focusing on aspects such as cellular senescence, chromosomal stability, tumorigenicity, and microbial contamination. In this study, using SFM to culture cells did not accelerate the senescence of hUC-MSCs compared to SCM. Interestingly, as the culture duration increases, different SFM formulations exhibited varying rates of cellular senescence, with cells cultured in SFM1 displaying the slowest rate, which suggested that additives added to the media could retard cellular senescence and provide valuable insights for future improvements in cell processing techniques. To obtain clinical-grade hUC-MSCs for future cell therapy, the cell manufacturing process, including donor screening, cell isolation, batch production, cryopreservation and thawing, requires rigorous monitoring to ensure biological safety, including detection of fungal and bacterial contamination, endotoxins, and pathogenic viruses. In this study, all four SFM-cultured hUC-MSCs showed negative results for fungal, endotoxin, and sterility testing. PCR testing of P5 and P10 generations of hUC-MSCs cultured in SFM revealed no contamination with HIV, cytomegalovirus, hepatitis B virus, hepatitis C virus, Epstein-Barr virus and human papilloma virus. Besides, soft agar cloning experiments revealed that hUC-MSCs cultured in the four SFM at passages 5 and 10 did not form colonies, while the positive control A549 and H1299 cells formed colonies. Furthermore, we found that prolonged cell culture to passage 10 did not induce chromosomal aberrations in hUC-MSCs. These results demonstrate that hUC-MSCs cultured in SFM are biologically safe.

Currently, there is no clear consensus on the maximum passages acceptable for clinical use of hUC-MSCs. In our study, if hUC-MSCs were cultured in SFM1 to 5 passage, a 40 cm long umbilical cord is expected to yield approximately  $1 \times 10^{12}$  cells, consuming approximately 2000 liters of culture media (20 ml media/T175 cell culture flask). If each infusion requires  $5 \times 10^7$  cells, the hUC-MSCs cultured in SFM1 would be sufficient for approximately 20000-times infusion.

It should be noted that although our research pointed out that the impact of different formulations of culture media on cell phenotype function may affect the therapeutic effect of subsequent diseases, more research and evidence are needed to explain what formulations should be used for different diseases. Determining the relationship between the compositions of the culture medium and cell function may promote the development of the cell therapy industry. Additionally, our findings highlight the importance of integrating culture medium selection with the overall stem cell production process and underscore the need for further research to determine how the production process impact the efficacy of cell-based therapies. From the perspective of the long-term development of the cell therapy industry, pharmaceutical companies that master the core culture media formulations will possess stronger core competitiveness, thereby helping them gain a competitive advantage in the field of cell therapy.

## Conclusions

In this study, we developed a strategy to obtain SFM and used it to formulate four SFM. We emphasize that, to the best of our knowledge, this is the first systematic comparison from an industrial perspective to evaluate the consistency of different culture media in producing clinical-grade hUC-MSCs. We propose that the clinical application of hUC-MSCs requires careful selection of culture media. One possible effective approach is to screen and select suitable culture media based on the characteristics of the specific disease being targeted for treatment. Developers of clinical applications for hUC-MSCs can also utilize the strategy outlined in this study to establish their customized SFM research platform to investigate and obtain hUC-MSCs targeted specific diseases. This represents a significant step forward in promoting the implementation of stem cell therapy from scientific research to large-scale industry application.

## Abbreviations

hUC-MSCs	Umbilical cord mesenchymal stem cells
SFM	Serum-Free media
SCM	Serum-Containing media
MSCs	Stem/Stromal cells
ISCT	Society of cellular therapy
GMP	Manufacturing practice

FBS	Bovine serum
PDT	Doubling time
PPL	Proliferative level of logarithmic growth phase cells
CD	Cluster of differentiation
PI	Propidium iodide
UC	Umbilical cord
HIV	Human immunodeficiency virus
CMV	Cytomegalovirus
HBV	Human hepatitis B virus
HCV	Human hepatitis C virus
EBV	Epstein-Barr virus
HPV	Human papilloma virus
FACS	Fluorescence-activated cell sorting
CAFC	Cobblestone area-forming cells
HSC	Hemopoietic stem cell
UCB	Umbilical cord blood
PFA	Polyformaldehyde

## Supplementary Information

The online version contains supplementary material available at <https://doi.org/10.1186/s13287-024-03949-0>.

Supplementary Material 1: Figure S1. Tumorigenicity test of hUC-MSCs in different SFM. P5 and P10 passages of hUC-MSCs cultured in customized SFM were utilized to evaluate the tumorigenicity.

Supplementary Material 2: Figure S2. The senescence status of hUC-MSCs cultured with different media. hUC-MSCs were cultured in SFM and SCM to corresponding passages, and the cellular senescence status was assessed using  $\beta$ -galactosidase staining. The  $\beta$ -gal-positive cells are indicated by the red arrows.

Supplementary Material 3: Figure S3. The proliferation curves of cells at passage 5 and 10. Cells from passages P4 or P9 were seeded into a 24-well plate. Cell number at indicated time points were assessed by trypan blue staining. Results are expressed as means  $\pm$  SEM. \*  $p < 0.05$ ; \*\*  $p < 0.01$ ; \*\*\*  $p < 0.001$ ; \*\*\*\*  $p < 0.0001$ .

Supplementary Material 4: Figure S4. Analysis of the cell cycle in P5 and P10 of hUC-MSCs. hUC-MSCs from P5 and P10 were harvested for cell cycle analysis. The proportions of S and G2/M stages of hUC-MSCs cultured in customized media were analyzed by FACS.

Supplementary Material 5: Figure S5. The effects of cryopreservation and resuscitation on cell activity and proliferation. hUC-MSCs were cultured in SCM1 (A), SCM2 (B), SFM1 (C), SFM2 (D), and SFM3 (E) to indicated passages. Cell viability, multiple increase and PDT of cryopreservation and thawing (cryo-thawing) hUC-MSCs were determined before and after cryopreservation. Results shown in A-E are expressed as means  $\pm$  SEM.

## Acknowledgements

Not applicable.

## Author contributions

LJ Bi and L Zhao conceived and designed the experiments. L Zhao and BB Ni performed the experiments. JQ Li, WJ Yang and W Yu analysed the data. L Zhao and BB Ni wrote the paper. R Liu, Q Zhang and ZB Zheng collected UC samples.

## Funding

The work was supported by the project grants from the Young Scientists Program of Guangzhou Laboratory (No. QNPG24-09), the Science Assistance Project for Xinjiang (2024E02062), the National Natural Science Foundation of China (32394014, 82304575) and Guangdong Provincial Basic and Applied Basic Research Fund (2022A151110883).

## Availability of data and materials

All data relevant to the study are included in the article or uploaded as supplementary information.

## Declarations

### Ethics approval and consent to participate

This study has been approved by the Ethics Committee of The Third Affiliated Hospital of Sun Yat-sen University. Informed consent was obtained from healthy donors prior to the collection of UCs. The research project titled "Multi-center randomized controlled clinical study of allogeneic human umbilical cord mesenchymal stem cells in the treatment of hepatitis B related chronic and acute liver dysfunction" was approved on December 30, 2020 (approval number: 202014).

### Consent for publication

Not applicable.

### Competing interests

The authors declare that they have no competing interests.

### Author details

<sup>1</sup>Guangzhou National Laboratory, Guangzhou 510005, People's Republic of China. <sup>2</sup>Vaccine Research Institute, Cell-Gene Therapy Translational Medicine Research Centre, The Third Affiliated Hospital of Sun Yat-sen University, Guangzhou 510630, People's Republic of China. <sup>3</sup>Division of Hematology and Oncology, Department of Geriatrics, Guangzhou First People's Hospital, School of Medicine, South China University of Technology, Guangzhou 510180, People's Republic of China. <sup>4</sup>Department of Hematology, Sun Yat-sen Memorial Hospital, Sun Yat-sen University, Guangzhou 510120, People's Republic of China.

Received: 26 June 2024 Accepted: 18 September 2024

Published online: 27 September 2024

## References

- Li P, Ou Q, Shi S, Shao C. Immunomodulatory properties of mesenchymal stem cells/dental stem cells and their therapeutic applications. *Cell Mol Immunol*. 2023;20(6):558–69.
- Izadi M, Sadr Hashemi Nejad A, Moazenchi M, Masoumi S, Rabbani A, Kompani F, Hedayati Asl AA, Abbasi Kakroodi F, Jaroughi N, Mohseni Meybodi MA, Setoodeh A, Abbasi F, Hosseini SE, Moeini Nia F, Salman Yazdi R, Navabi R, Hajjizadeh-Saffar E, Baharvand H. Mesenchymal stem cell transplantation in newly diagnosed type-1 diabetes patients: a phase I/II randomized placebo-controlled clinical trial. *Stem Cell Res Ther*. 2022;13(1):264.
- Li Q, Hou H, Li M, Yu X, Zuo H, Gao J, Zhang M, Li Z, Guo Z. CD73<sup>+</sup> mesenchymal stem cells ameliorate myocardial infarction by promoting angiogenesis. *Front Cell Dev Biol*. 2021;12(9):637239.
- Nie M, Kong B, Chen G, Xie Y, Zhao Y, Sun L. MSCs-laden injectable self-healing hydrogel for systemic sclerosis treatment. *Bioact Mater*. 2022;19(17):369–78.
- Wang W, Zhang M, Ren X, Song Y, Xu Y, Zhuang K, Xiao T, Guo X, Wang S, Hong Q, Feng Z, Chen X, Cai G. Single-cell dissection of cellular and molecular features underlying mesenchymal stem cell therapy in ischemic acute kidney injury. *Mol Ther*. 2023;31(10):3067–83.
- Beetler DJ, Di Florio DN, Law EW, Groen CM, Windebank AJ, Peterson QP, Fairweather D. The evolving regulatory landscape in regenerative medicine. *Mol Aspects Med*. 2023;91:101138.
- López-Beas J, Guadix JA, Clares B, Soriano-Ruiz JL, Zugaza JL, Gálvez-Martín P. An overview of international regulatory frameworks for mesenchymal stromal cell-based medicinal products: from laboratory to patient. *Med Res Rev*. 2020;40(4):1315–34.
- Al-Azab M, Idiattullina E, Safi M, Hezam K. Enhancers of mesenchymal stem cell stemness and therapeutic potency. *Biomed Pharmacother*. 2023;162:114356.
- Mönch D, Reinders MEJ, Dahlke MH, Hoogduijn MJ. How to make sense out of 75,000 mesenchymal stromal cell publications? *Cells*. 2022;11(9):1419.
- Bahari M, Mokhtari H, Yeganeh F. Stem cell therapy, the market, the opportunities and the threat. *Int J Mol Cell Med*. 2023;12(3):310–9.
- Hoang DM, Pham PT, Bach TQ, Ngo ATL, Nguyen QT, Phan TTK, Nguyen GH, Le PTT, Hoang VT, Forsyth NR, Heke M, Nguyen LT. Stem cell-based therapy for human diseases. *Signal Transduct Target Ther*. 2022;7(1):272.
- Bui HTH, Nguyen LT, Than UTT. Influences of Xeno-free media on mesenchymal stem cell expansion for clinical application. *Tissue Eng Regen Med*. 2021;18(1):15–23.
- Agostini F, Vicinanza C, Lombardi E, Da Ros F, Marangon M, Massarut S, Mazzucato M, Durante C. Ex vivo expansion in a clinical grade medium, containing growth factors from human platelets, enhances migration capacity of adipose stem cells. *Front Immunol*. 2024;14(15):1404228.
- Winkel A, Jaimes Y, Melzer C, Dillschneider P, Hartwig H, Stiesch M, von der Ohe J, Strauss S, Vogt PM, Hamm A, Burmeister L, Roger Y, Elger K, Floerkemeier T, Weissinger EM, Pogozhykh O, Müller T, Selich A, Rothe M, Petri S, Köhl U, Hass R, Hoffmann A. Cell culture media notably influence properties of human mesenchymal stroma/stem-like cells from different tissues. *Cytotherapy*. 2020;22(11):653–68.
- Nagasaki K, Nakashima A, Tamura R, Ishiuchi N, Honda K, Ueno T, Doi S, Kato Y, Masaki T. Mesenchymal stem cells cultured in serum-free medium ameliorate experimental peritoneal fibrosis. *Stem Cell Res Ther*. 2021;12(1):203.
- Ullah I, Subbarao RB, Rho GJ. Human mesenchymal stem cells—current trends and future prospective. *Biosci Rep*. 2015;35(2):e00191.
- Lv FJ, Tuan RS, Cheung KM, Leung VY. Concise review: the surface markers and identity of human mesenchymal stem cells. *Stem Cells*. 2014;32(6):1408–19.
- Mushahary D, Spittler A, Kasper C, Weber V, Charwat V. Isolation, cultivation, and characterization of human mesenchymal stem cells. *Cytom A*. 2018;93(1):19–31.
- Ghaneialvar H, Soltani L, Rahmani HR, Lotfi AS, Soleimani M. Characterization and classification of mesenchymal stem cells in several species using surface markers for cell therapy purposes. *Indian J Clin Biochem*. 2018;33(1):46–52.
- Dominici M, Le Blanc K, Mueller I, Slaper-Cortenbach I, Marini F, Krause D, Deans R, Keating A, Prockop D, Horwitz E. Minimal criteria for defining multipotent mesenchymal stromal cells. The international society for cellular therapy position statement. *Cytotherapy*. 2006;8(4):315–7.
- Swamynathan P, Venugopal P, Kannan S, Thej C, Kolkundar U, Bhagwat S, Ta M, Majumdar AS, Balasubramanian S. Are serum-free and xeno-free culture conditions ideal for large scale clinical grade expansion of Wharton's jelly derived mesenchymal stem cells? A comparative study. *Stem Cell Res Ther*. 2014;5(4):88.
- Czapla J, Matuszczak S, Kulik K, Wiśniewska E, Pilny E, Jarosz-Biej M, Smolarczyk R, Sirek T, Zembala MO, Zembala M, Szala S, Cichoń T. The effect of culture media on large-scale expansion and characteristic of adipose tissue-derived mesenchymal stromal cells. *Stem Cell Res Ther*. 2019;10(1):235.
- Piletz JE, Drivon J, Eisenga J, Buck W, Yen S, McClin M, Meruvia W, Amaral C, Brue K. Human cells grown with or without substitutes for fetal bovine serum. *Cell Med*. 2018;6(10):2155179018755140.
- Selvaggi TA, Walker RE, Fleisher TA. Development of antibodies to fetal calf serum with arthus-like reactions in human immunodeficiency virus-infected patients given syngeneic lymphocyte infusions. *Blood*. 1997;89(3):776–9.
- Tuschong L, Soenen SL, Blaese RM, Candotti F, Muul LM. Immune response to fetal calf serum by two adenosine deaminase-deficient patients after T cell gene therapy. *Hum Gene Ther*. 2002;13(13):1605–10.
- Santos Fd, Andrade PZ, Abecasis MM, Gimble JM, Chase LG, Campbell AM, Boucher S, Vemuri MC, Silva CL, Cabral JM. Toward a clinical-grade expansion of mesenchymal stem cells from human sources: a microcarrier-based culture system under xeno-free conditions. *Tissue Eng Part C Methods*. 2011;17(12):1201–10.
- Chase LG, Yang S, Zachar V, Yang Z, Lakshminpathy U, Bradford J, Boucher SE, Vemuri MC. Development and characterization of a clinically compliant xeno-free culture medium in good manufacturing practice for human multipotent mesenchymal stem cells. *Stem Cells Transl Med*. 2012;1(10):750–8.
- Bucar S, Branco ADM, Mata MF, Milhano JC, Caramalho Í, Cabral JMS, Fernandes-Platzgummer A, da Silva CL. Influence of the mesenchymal stromal cell source on the hematopoietic supportive capacity of umbilical cord blood-derived CD34<sup>+</sup>-enriched cells. *Stem Cell Res Ther*. 2021;12(1):399.

29. Denning-Kendall P, Singha S, Bradley B, Hows J. Cobblestone area-forming cells in human cord blood are heterogeneous and differ from long-term culture-initiating cells. *Stem Cells*. 2003;21(6):694–701.
30. Pal R, Hanwate M, Jan M, Totev S. Phenotypic and functional comparison of optimum culture conditions for upscaling of bone marrow-derived mesenchymal stem cells. *J Tissue Eng Regen Med*. 2009;3(3):163–74.
31. Tonarova P, Lochovska K, Pytlík R, Hubalek KM. The impact of various culture conditions on human mesenchymal stromal cells metabolism. *Stem Cells Int*. 2021;1(2021):6659244.
32. Bhat S, Viswanathan P, Chandanala S, Prasanna SJ, Seetharam RN. Expansion and characterization of bone marrow derived human mesenchymal stromal cells in serum-free conditions. *Sci Rep*. 2021;11(1):3403.
33. Zhao K, Liu Q. The clinical application of mesenchymal stromal cells in hematopoietic stem cell transplantation. *J Hematol Oncol*. 2016;9(1):46.
34. Le Blanc K, Samuelsson H, Gustafsson B, Remberger M, Sundberg B, Arvidson J, Ljungman P, Lönnies H, Nava S, Ringdén O. Transplantation of mesenchymal stem cells to enhance engraftment of hematopoietic stem cells. *Leukemia*. 2007;21(8):1733–8.
35. Zhao L, Chen S, Yang P, Cao H, Li L. The role of mesenchymal stem cells in hematopoietic stem cell transplantation: prevention and treatment of graft-versus-host disease. *Stem Cell Res Ther*. 2019;10(1):182.
36. Arango-Rodríguez ML, Mateus LC, Sossa CL, Becerra-Bayona SM, Solarte-David VA, Ochoa Vera ME, Viviescas LTG, Berrio AMV, Serrano SE, Vargas O, Isla AC, Benitez A, Rangel G. A novel therapeutic management for diabetes patients with chronic limb-threatening ischemia: comparison of autologous bone marrow mononuclear cells versus allogenic Wharton jelly-derived mesenchymal stem cells. *Stem Cell Res Ther*. 2023;14(1):221.
37. Pan L, Liu C, Liu Q, Li Y, Du C, Kang X, Dong S, Zhou Z, Chen H, Liang X, Chu J, Xu Y, Zhang Q. Human Wharton's jelly-derived mesenchymal stem cells alleviate conavalin A-induced fulminant hepatitis by repressing NF- $\kappa$ B signaling and glycolysis. *Stem Cell Res Ther*. 2021;12(1):496.
38. Cheng T, Ding S, Liu S, Li Y, Sun L. Human umbilical cord-derived mesenchymal stem cell therapy ameliorates lupus through increasing CD4<sup>+</sup> T cell senescence via MiR-199a-5p/Sirt1/p53 axis. *Theranostics*. 2021;11(2):893–905.
39. Gupta A, Maffulli N, Rodriguez HC, Lee CE, Levy HJ, El-Amin SF 3rd. Umbilical cord-derived Wharton's jelly for treatment of knee osteoarthritis: study protocol for a non-randomized, open-label, multi-center trial. *J Orthop Surg Res*. 2021;16(1):143.
40. Yip HK, Fang WF, Li YC, Lee FY, Lee CH, Pei SN, Ma MC, Chen KH, Sung PH, Lee MS. Human umbilical cord-derived mesenchymal stem cells for acute respiratory distress syndrome. *Crit Care Med*. 2020;48(5):e391–9.
41. Galbraith SC, Bhatia H, Liu H, et al. Media formulation optimization: current and future opportunities. *Curr Opin Chem Eng*. 2018;22:42–7.
42. Wei Z, Batagov AO, Carter DR, Krichevsky AM. Fetal bovine serum RNA interferes with the cell culture derived extracellular RNA. *Sci Rep*. 2016;9(6):31175.
43. Gottipamula S, Muttigi MS, Kolkundkar U, Seetharam RN. Serum-free media for the production of human mesenchymal stromal cells: a review. *Cell Prolif*. 2013;46(6):608–27.
44. Panella S, Muoio F, Jossen V, et al. Chemically defined xeno-and serum-free cell culture medium to grow human adipose stem cells. *Cells*. 2021;10(2):466.
45. Park J, Lee JH, Yoon BS, Jun EK, Lee G, Kim IY, You S. Additive effect of bFGF and selenium on expansion and paracrine action of human amniotic fluid-derived mesenchymal stem cells. *Stem Cell Res Ther*. 2018;9(1):293.
46. Schmidt A, Ladage D, Schinköthe T, Klausmann U, Ulrichs C, Klinz FJ, Brixius K, Arnhold S, Desai B, Mehlhorn U, Schwinger RH, Staib P, Addicks K, Bloch W. Basic fibroblast growth factor controls migration in human mesenchymal stem cells. *Stem Cells*. 2006;24(7):1750–8.
47. Hosseinzadeh Anvar L, Hosseini-Asl S, Mohammadzadeh-Vardin M, Sagha M. The telomerase activity of selenium-induced human umbilical cord mesenchymal stem cells is associated with different levels of c-Myc and p53 expression. *DNA Cell Biol*. 2017;36(1):34–41.
48. Taurino G, Deshmukh R, Villar VH, Chiu M, Shaw R, Hedley A, Shokry E, Sumpton D, Dander E, D'Amico G, Bussolati O, Tardito S. Mesenchymal stromal cells cultured in physiological conditions sustain citrate secretion with glutamate anaplerosis. *Mol Metab*. 2022;63:101532.
49. Al Masawa ME, Wan Kamarul Zaman WS, Chua KH. Biosafety evaluation of culture-expanded human chondrocytes with growth factor cocktail: a preclinical study. *Sci Rep*. 2020;10(1):21583.
50. Astori G, Amati E, Bambi F, Bernardi M, Chieregato K, Schäfer R, Sella S, Rodeghiero F. Platelet lysate as a substitute for animal serum for the ex vivo expansion of mesenchymal stem/stromal cells: present and future. *Stem Cell Res Ther*. 2016;7(1):93.
51. Azouna NB, Jenhani F, Regaya Z, Berraes L, Othman TB, Ducrocq E, Domenech J. Phenotypical and functional characteristics of mesenchymal stem cells from bone marrow: comparison of culture using different media supplemented with human platelet lysate or fetal bovine serum. *Stem Cell Res Ther*. 2012;3(1):6.
52. Chevallier N, Anagnostou F, Zilber S, Bodivit G, Maurin S, Barrault A, Bierling P, Hernigou P, Layrolle P, Rouard H. Osteoblastic differentiation of human mesenchymal stem cells with platelet lysate. *Biomaterials*. 2010;31(2):270–8.
53. Rhee Y-H, Choi M, Lee H-S, Park C-H, Kim S-M, Yi S-H, Oh S-M, Cha H-J, Chang M-Y, Lee S-H. Insulin concentration is critical in culturing human neural stem cells and neurons. *Cell Death Dis*. 2013;4(8):e766.
54. Yoo HC, Yu YC, Sung Y, Han JM. Glutamine reliance in cell metabolism. *Exp Mol Med*. 2020;52(9):1496–516.
55. Saito Y, Yoshida Y, Akazawa T, Takahashi K, Niki E. Cell death caused by selenium deficiency and protective effect of antioxidants. *J Biol Chem*. 2003;278(41):39428–34.
56. Gao M, Monian P, Quadri N, Ramasamy R, Jiang X. Glutaminolysis and transferrin regulate ferroptosis. *Mol Cell*. 2015;59(2):298–308.
57. Kabat M, Bobkov I, Kumar S, Grumet M. Trends in mesenchymal stem cell clinical trials 2004–2018: is efficacy optimal in a narrow dose range? *Stem Cells Transl Med*. 2020;9(1):17–27.
58. Cao TT, Chen H, Pang M, Xu SS, Wen HQ, Liu B, Rong LM, Li MM. Dose optimization of intrathecal administration of human umbilical cord mesenchymal stem cells for the treatment of subacute incomplete spinal cord injury. *Neural Regen Res*. 2022;17(8):1785–94.
59. Eydzian Z, Mohammad Ghasemi A, Ansari S, Kamali AN, Khosravi M, Momtaz S, Riki S, Rafighdoost L, Entezari HR. Differentiation of multipotent stem cells to insulin-producing cells for treatment of diabetes mellitus: bone marrow- and adipose tissue-derived cells comparison. *Mol Biol Rep*. 2022;49(5):3539–48.
60. Ménard C, Dulong J, Roulois D, Hébraud B, Verdière L, Pangault C, Sibut V, Bezier I, Bescher N, Monvoisin C, Gadelorge M, Bertheuil N, Flécher E, Casteilla L, Collas P, Sensebé L, Bourin P, Espagnolle N, Tarte K. Integrated transcriptomic, phenotypic, and functional study reveals tissue-specific immune properties of mesenchymal stromal cells. *Stem Cells*. 2020;38(1):146–59.
61. Nakao M, Inanaga D, Nagase K, Kanazawa H. Characteristic differences of cell sheets composed of mesenchymal stem cells with different tissue origins. *Regen Ther*. 2019;10(11):34–40.
62. Donders R, Bogie JFJ, Ravanidis S, Gervois P, Vanheusden M, Marée R, Schrynmackers M, Smeets HJM, Pinxteren J, Gijbels K, Walbers S, Mays RW, Deans R, Van Den Bosch L, Stinissen P, Lambrichts I, Gyselaers W, Hellings N. Human Wharton's jelly-derived stem cells display a distinct immunomodulatory and proregenerative transcriptional signature compared to bone marrow-derived stem cells. *Stem Cells Dev*. 2018;27(2):65–84.
63. Thakkar UG, Trivedi HL, Vanikar AV, Dave SD. Insulin-secreting adipose-derived mesenchymal stromal cells with bone marrow-derived hematopoietic stem cells from autologous and allogenic sources for type 1 diabetes mellitus. *Cytotherapy*. 2015;17(7):940–7.
64. Fekete N, Rojewski MT, Fürst D, Kreja L, Ignatius A, Dausend J, Schrezenmeier H. GMP-compliant isolation and large-scale expansion of bone marrow-derived MSC. *PLoS ONE*. 2012;7(8):e43255.
65. Heathman TR, Glyn VA, Picken A, Rafiq QA, Coopman K, Nienow AW, Kara B, Hewitt CJ. Expansion, harvest and cryopreservation of human mesenchymal stem cells in a serum-free microcarrier process. *Biotechnol Bioeng*. 2015;112(8):1696–707.
66. Crapnell K, Blaesusius R, Hastings A, Lennon DP, Caplan AI, Bruder SP. Growth, differentiation capacity, and function of mesenchymal stem cells expanded in serum-free medium developed via combinatorial screening. *Exp Cell Res*. 2013;319(10):1409–18.
67. Wu X, Kang H, Liu X, Gao J, Zhao K, Ma Z. Serum and xeno-free, chemically defined, no-plate-coating-based culture system for mesenchymal stromal cells from the umbilical cord. *Cell Prolif*. 2016;49(5):579–88.

68. Youssef A, Han VK. Low oxygen tension modulates the insulin-like growth factor-1 or -2 signaling via both insulin-like growth factor-1 receptor and insulin receptor to maintain stem cell identity in placental mesenchymal stem cells. *Endocrinology*. 2016;157(3):1163–74.
69. Youssef A, Iosef C, Han VK. Low-oxygen tension and IGF-I promote proliferation and multipotency of placental mesenchymal stem cells (PMSCs) from different gestations via distinct signaling pathways. *Endocrinology*. 2014;155(4):1386–97.
70. Ben Azouna N, Jenhani F, Regaya Z, Berraies L, Ben Othman T, Ducrocq E, Domenech J. Phenotypical and functional characteristics of mesenchymal stem cells from bone marrow: comparison of culture using different media supplemented with human platelet lysate or fetal bovine serum. *Stem Cell Res Ther*. 2012;3(1):6.
71. Stern-Straeter J, Bonaterra GA, Juritz S, Birk R, Goessler UR, Bieback K, Bugert P, Schultz J, Hörmann K, Kinscherf R, Faber A. Evaluation of the effects of different culture media on the myogenic differentiation potential of adipose tissue- or bone marrow-derived human mesenchymal stem cells. *Int J Mol Med*. 2014;33(1):160–70.

### **Publisher's Note**

Springer Nature remains neutral with regard to jurisdictional claims in published maps and institutional affiliations.